Phase transition and crossover in diffusion-limited aggregation with reaction times

Takashi Nagatani
College of Engineering, Shizuoka University, Hamamatsu 432, Japan
and Center for Polymer Studies and Department of Physics, Boston University, Boston, Massachusetts 02215

H. Eugene Stanley
Center for Polymer Studies and Department of Physics, Boston University, Boston, Massachusetts 02215
(Received 25 May 1990)

A generalized diffusion-limited aggregation (DLA) with reaction times that has been proposed by Bunde and Miyazima [Phys. Rev. A **38**, 2099 (1988)] is considered. Crossover from the DLA to the diffusion-limited self-avoiding walk (DLSAW) is investigated by using the two-parameter position-space renormalization-group method. The crossover exponent and the crossover radius are calculated. The geometrical phase transition between DLA and DLSAW found by Bunde and Miyajima is analyzed by making use of the three-parameter position-space renormalization-group method. A global flow diagram in the three-parameter space is obtained. Above the percolation threshold all the renormalization flows are merged into the DLA point. Below the threshold all the renormalization flows are merged into the DLSAW point. When the reaction time is large, the double-crossover phenomenon occurs below the threshold.

I. INTRODUCTION

Fractal growth phenomena in pattern formation have recently attracted considerable attention.[1-11] Examples of pattern formation in diffusive systems include viscous fingering, electrochemical deposition, crystal growth, and dielectric breakdown. The fractal nature of the aggregate has been analyzed by computational, experimental, and analytic methods. Several approaches to simple generalizations of the diffusion-limited aggregation (DLA) model have been carried out to take into account sticking probability, surface tension, particle drift, multiparticle effects, and lifetime effects. The crossover phenomena and the geometrical phase transition between the DLA fractal and the nonfractals have been found by computational and experimental methods. The effect of the lifetime on the fractal nature of DLA has been studied by the computer simulation.[12,13] Miyajima *et al.*[12] found the crossover from the DLA fractal to the diffusion-limited self-avoiding walk[14] (DLSAW) in a generalized DLA model where all the aggregate sites have a finite radical time. Bunde and Miyajima[13] furthermore found the geometrical phase transition in the extended DLA model in which each aggregate site is randomly assigned an infinite reaction time (with probability P) or a finite reaction time (with probability $1-P$). The extended DLA model reduces to the Witten-Sander model[1] for $P=1$ and to the model discussed by Miyajima *et al.*[12] for $P=0$. They found that the geometrical transition occurs at the percolation threshold $P=P_c$. The phase transition and the crossover have never been analyzed by analytical methods.

Very recently, Lee, Coniglio, and Stanley[15] succeeded in analyzing the crossover from the DLA fractal to the dense structure in viscous fingering at the finite viscosity ratio by using the two-parameter position-space renormalization-group method. Nagatani[16] analyzed the effect of the sticking probability on the fractal nature of the DLA. When the sticking probability is small, the aggregate must eventually cross over to the DLA fractal. Furthermore, the combined effect of the sticking probability and the finite viscosity ratio was analyzed by using the three-parameter position-space renormalization-group method.[17] The double-crossover phenomena were found from the dense pattern, through the DLA fractal, to the dense structure. The renormalization-group approach will be a powerful tool in analyzing the morphological changes.

In this paper, we analyze the effect of the reaction time on the DLA by using a position-space renormalization-group method. We consider the two models proposed by Miyajima *et al.*[12] and Bunde and Miyajima.[13] In the first model, each aggregate particle has a finite reaction time τ: if a particle adheres to the aggregate at a certain time t_0, then incoming Brownian particles can adhere to sites adjacent to this particle only up to time $t_0+\tau$. In the second model, a fraction P of the particles has an infinite reaction time (as in the Witten-Sander model), with the remaining fraction $1-P$ having a finite reaction time. We show that at $P=0$ the crossover from the DLA fractal to the DLSAW occurs. We also show that at the percolation threshold the geometrical transition between the DLA fractal and the DLSAW occurs.

The organization of the paper is as follows. In Sec. II we analyze the crossover phenomenon from the DLA fractal to the DLSAW in a generalized DLA model proposed by Miyajima *et al.*[12] by using the two-parameter position-space renormalization-group method. In Sec. III we analyze the geometrical phase transition between the DLA fractal and the DLSAW. In Sec. IV we present the summary.

II. CROSSOVER PHENOMENON

We consider a generalized DLA model where aggregate sites have a finite radical time. The model was proposed by Miyajima *et al.*[12] The crossover phenomenon from the DLA fractal to the DLSAW was found by computer simulation. We apply the position-space renormalization-group method to the DLA model where all the sites of the aggregate have a finite reaction time. Each aggregate particle has a finite reaction time τ: if a particle adheres to the aggregate at a certain time t_0, then incoming Brownian particles can adhere to sites adjacent to this particle only up to time $t_0+\tau$. We define A_i, the activity of the perimeter site i,

$$A_i((t-t_0)/\tau)=\begin{cases}1 & \text{if } (t-t_0)/\tau\le 1\\ 0 & \text{if } (t-t_0)/\tau>1\end{cases}, \tag{1}$$

where t_0 is the time in which a particle sticks on the perimeter site i, and τ the reaction time. Furthermore, we define the dimensionless time increment Δt^* as follows:

$$\Delta t^*=(t-t_0)/\tau\ . \tag{2}$$

The growth probability p_i on the perimeter site i is given by

$$p_i=A_i\bar{p}_i\Big/\sum_i A_i\bar{p}_i\ , \tag{3}$$

where $\bar{p}_i$ is the growth probability on the perimeter site i with an infinite reaction time. We describe the DLA problem in terms of the dielectric breakdown model. We consider the renormalization procedure on the diamond hierarchical lattice.[18] Each bond is occupied by a resistor of unit conductance. A constant voltage is applied between the bottom and the top on the diamond hierarchical lattice. We shall derive the renormalization-group equations for the surface conductance and the dimensionless time increment. See Ref. 18 for details of the renormalization-group method. We distinguish between three types of bonds on the lattice before and after a renormalization: (i) breakdown bonds constructing the breakdown pattern, (ii) growth bonds on the perimeter of the breakdown pattern, and (iii) unbroken bonds consisting of the original resistor. The breakdown, growth, and unbroken bonds are, respectively, indicated by the thick, wavy, and thin lines in the Fig. 1. We partition all the space of the diamond lattice into cells of size $b=2$ (b is the scale factor), each containing a single generator. After a renormalization transformation these cells play the role of "renormalized" bonds. The nth generation of the diamond lattice is transformed to the $(n-1)$th generation. The renormalized bonds are then classified into the three types of bonds, similarly to the bond before renormalization. The conductance of the unbroken bond after renormalization remains a unit value. The conductance of the renormalized bond as the growth bond is transformed to a different value after renormalization. We assign an "effective conductance" for the growth bond on the perimeter. If the bond on the nth generation is the growth bond, then the effective conductance is assigned to be σ_s. Then the conductance of the cell to be renormalized as the growth bond is renormalized to σ_s'. We call the conductance σ_s the surface conductance. The renormalization transformation of the surface conductance constitutes the first of the renormalization equations:

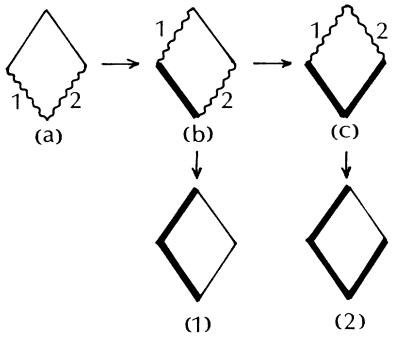

FIG. 1. All distinct configurations of the cell. The configurations (a), (b), and (c) are renormalized to the growth bonds. The configurations (1) and (2) are renormalized to the breakdown bonds. The thick, wavy, and thin lines indicate breakdown, growth, and unbroken bonds, respectively.

$$\sigma_s'=R_s(\sigma_s,\Delta t^*)\ . \tag{4}$$

The breakdown process occurs one by one. The time increment Δt is defined to be the time period between breakdown of one bond and breakdown of the next bond. The time increment Δt is renormalized to be the time period $\Delta t'$ in which the breakdown proceeds from the bottom to the top within the cell. The cell is a spanning cluster in which the top is connected with the bottom by the breakdown bonds. The cell is renormalized to the breakdown bond. The renormalization transformation of the dimensionless time increment constitutes the second of the renormalization equations:

$$\Delta t^{*'}=R_t(\sigma_s,\Delta t^*)\ . \tag{5}$$

Equations (4) and (5) give the renormalization-group equations. We derive the renormalization functions (4) and (5) explicitly. Figure 1 shows the breakdown process within the cell. We assume that the breakdown process occurs stepwise: the breakdown proceeds one by one, and only one bond breaks at a time (there is no simultaneous bond breaking). The configuration in Fig. 1(a) shows the cell in which the breakdown just reaches at the bottom. The configuration in Fig. 1(b) is constructed by adding a breakdown bond onto the growth bonds 1 or 2 in configuration (a). The probability with which a breakdown bond adds onto the growth bonds 1 or 2 in configuration (a) is given by the growth probabilities $p_{a,1}$ or $p_{a,2}$ of the growth bonds 1 or 2 in configuration (a). In addition, by adding a breakdown bond to configuration (b), the configurations (c) and (1) occur. Furthermore, by proceeding to the breakdown, the configuration (2) occurs. The configurations (a)–(c) in Fig. 1 show all the configurations of the cell for which it is possible to renormalize as the growth bond. The configurations (1) and (2) show the spanning clusters to be renormalized as the

breakdown bond. Parts (1) and (2) in Fig. 1 give all the configurations of the spanning cluster. Let us consider the configurational probability C_α with which a particular configuration α appears. The distinct configurations are labeled by α (α=a,b,c,1,2) in Fig. 1. Here the configurational probabilities are normalized, respectively, as 1 for the renormalized growth bonds and the renormalized breakdown bonds. The configurational probabilities C_α (α=a,b,c) are given by (see Ref. 8 for details)

$$\begin{aligned} C_{\rm a}&=1-C_{\rm b}-C_{\rm c}\ , \\ C_{\rm b}&=C_{\rm a}(p_{{\rm a},1}+p_{{\rm a},2})\ , \\ C_{\rm c}&=C_{\rm b}p_{{\rm b},2}\ , \end{aligned} \tag{6}$$

where $p_{\alpha,i}$ is the growth probability of the growth bond i within the cell α. the growth probability $p_{\alpha,i}$ on the growth bond i within the cell α is proportional to the current multiplied by the activity $A_{\alpha,i}$ on the growth bond. They are given by

$$\begin{aligned} &p_{{\rm a},1}=p_{{\rm a},2}=\tfrac{1}{2}\ , \\ &p_{{\rm b},1}=A_{{\rm b},1}\bar{p}_{{\rm b},1}/\sum_i A_{{\rm b},i}\bar{p}_{{\rm b},i}=\bar{p}_{{\rm b},1}/(\bar{p}_{{\rm b},1}+A\bar{p}_{{\rm b},2})\ , \\ &p_{{\rm b},2}=1-p_{{\rm b},1}\ , \\ &p_{{\rm c},1}=A_{{\rm c},1}\bar{p}_{{\rm c},1}/\sum_i A_{{\rm c},i}\bar{p}_{{\rm c},i}=A\bar{p}_{{\rm c},1}/(A\bar{p}_{{\rm c},1}+\bar{p}_{{\rm c},2})\ , \\ &p_{{\rm c},2}=1-p_{{\rm c},1}\ , \end{aligned} \tag{7}$$

where $\bar{p}_{{\rm b},1}=\sigma_s/[\sigma_s+(1+\sigma_s^{-1})^{-1}]$, $\bar{p}_{{\rm b},2}=1-\bar{p}_{{\rm b},1}$, $\bar{p}_{{\rm c},1}=\frac{1}{2}$, $\bar{p}_{{\rm c},2}=\frac{1}{2}$, and $A=A(\Delta t/\tau)$. Here Δt indicates the time period between the breakdown of one bond and the breakdown of the next bond. The configurations (1) and (2) in Fig. 1 show all the spanning clusters. Configurations (1) and (2) of the spanning cluster on the bottom side are constructed from the configurations of the growth cell on the top side. The configuration (1) is constructed by adding the breakdown bond onto the growth bond 1 in the configuration (b). The configurational probability C_1 of configuration (1) is given by

$$C_1=C_0p_{{\rm b},1}C_{\rm b}\ . \tag{8}$$

The configuration (2) is constructed by adding the breakdown bond onto the growth bonds 1 or 2 in the configuration (c). The configurational probability C_2 is given by

$$C_2=C_0C_{\rm c}\ . \tag{9}$$

The unknown constant C_0 is determined by the normalization condition

$$C_1+C_2=1\ . \tag{10}$$

The surface conductance $\sigma'_{s,\alpha}$ of the cell with the configuration α is renormalized as follows:

$$\begin{aligned} \sigma'_{s,{\rm a}}&=2\sigma_s/(1+\sigma_s)\ , \\ \sigma'_{s,{\rm b}}&=\sigma_s+\sigma_s/(1+\sigma_s)\ , \\ \sigma'_{s,{\rm c}}&=2\sigma_s\ . \end{aligned} \tag{11}$$

The renormalized conductance σ'_s of the growth bond will be assumed to be given by the most probable value

$$\sigma'_s=\exp(C_{\rm a}\ln\sigma'_{s,{\rm a}}+C_{\rm b}\ln\sigma'_{s,{\rm b}}+C_{\rm c}\ln\sigma'_{s,{\rm c}})\ . \tag{12}$$

Relationships (11) and (12) present the renormalization equation (4). In the limit of the infinite reaction time ($A=1$), Eqs. (11) and (12) reduce to those of the Witten-Sander model.[18] We consider the renormalization of the dimensionless time increment. The time increment Δt is renormalized to be the time period $\Delta t'$ in which the breakdown proceeds from the bottom to the top within the cell. Here the time increment is defined to be the time period between the breakdown of one bond and the breakdown of the next bond. The renormalized dimensionless time increments for the configurations (1) and (2) in Fig. 1 are given by

$$\begin{aligned} \Delta t_1^{*\prime}&=2\Delta t^*\ , \\ \Delta t_2^{*\prime}&=3\Delta t^*\ . \end{aligned} \tag{13}$$

The renormalized dimensionless time increment $\Delta t^{*'}$ will be assumed to be given by the mean value

$$\Delta t^{*'}=C_1\Delta t_1^{*\prime}+C_2\Delta t_2^{*\prime}\ . \tag{14}$$

Relationships (13) and (14) give the renormalization function $\Delta t^{*'}=R_t(\sigma_s,\Delta t^*)$. Equations (6)–(14) are simultaneously solved. We find the two nontrivial fixed points $(1/\sigma_{\rm DLA},0)$ and $(1/\sigma_{\rm DLSAW},1)$ in the parameter space $(1/\sigma_s,\Delta t^*/(1+\Delta t^*))$ where $\sigma_{\rm DLA}$ (=2.123) is the value of the fixed point in the limiting case of an infinite reaction time, and $\sigma_{\rm DLSAW}$ (=1.732) is the value of the fixed point in the limiting case of $\Delta t^*\to\infty$. In the limit of $\Delta t^*\to\infty$, the DLSAW fractal is reproduced. The fixed point $(1/\sigma_{\rm DLA},0)$ corresponds to the ordinary DLA model. It is called the DLA point. The fixed point $(1/\sigma_{\rm DLSAW},1)$ gives the DLSAW. It is called the DLSAW point. We study the stability of the fixed points in the two-parameter space $(1/\sigma_s,\Delta t^*/(1+\Delta t^*))$. To find the global flow diagram in the two-parameter space, we choose a point in the parameter space and calculate the renormalized surface conductance and the renormalized dimensionless time increment by using Eq. (4) and (5) to find a new point $(1/\sigma'_s,\Delta t^{*'}/(1+\Delta t^{*'}))$. We repeat this process to find the next point, and continue until we approach a stable fixed point. Figure 2 shows the renormalization flows. We can determine the stabilities of the two fixed points: the DLA point and the DLSAW point. The DLA point is an unstable fixed point. The DLSAW point is stable in every direction. All the renormalization flows eventually merge into the DLSAW point. It is found from the flow diagram that the crossover phenomenon occurs from the DLA fractal to the DLSAW fractal.

We propose the scaling ansatz along the crossover line

$$M(r,\Delta t^*)=r^{d_{\rm DLA}}F(\Delta t^* r^\phi)\ , \tag{15}$$

with

$$F(x)\approx\begin{cases}1 & \text{if } x\ll 1\\ x^{(d_{\rm DLSAW}-d_{\rm DLA})/\phi} & \text{if } x\gg 1\ ,\end{cases} \tag{16}$$

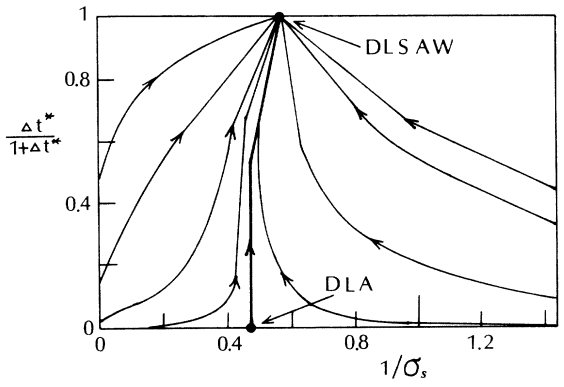

FIG. 2. Global flow diagram in the two-parameter space $(1/\sigma_s, \Delta t^*/(1+\Delta t^*))$. There are two fixed points: the DLA point and the DLSAW point. All the renormalization flows are eventually merged into the DLSAW point. The crossover occurs from the DLA fractal to the DLSAW fractal.

where M is the mass of the cluster, $F(x)$ is the scaling function, and d_{DLA} and d_{DLSAW} indicate, respectively, the fractal dimensions of the DLA and the DLSAW. By using the Turkevich-Scher relation,[19] the fractal dimensions are given by

$$d_{\mathrm{DLA}} = 1 + \ln p_{\max,\mathrm{DLA}} / \ln b = 1.40 ,$$
$$d_{\mathrm{DLSAW}} = 1 + \ln p_{\max,\mathrm{DLSAW}} / \ln b = 1 , \tag{17}$$

where $p_{\max,\mathrm{DLA}}$ and $p_{\max,\mathrm{DLSAW}}$ are, respectively, the highest growth probabilities at the DLA point and at the DLSAW. The crossover radius r_c scales as

$$r_c \approx (\Delta t^*)^{-1/\phi} . \tag{18}$$

The crossover exponent ϕ can be found by linearzing the renormalization equations (4) and (5) and calculating the eigenvalues. We obtain $\phi = 1.165$. For comparison with the computational result by Miyajima *et al.*,[12] we set $\Delta t = 1$ and obtain the scaling of the crossover time

$$t_c \approx r_c^{d_{\mathrm{DLA}}} \approx \tau^{d_{\mathrm{DLA}}/\phi} \quad \text{with } d_{\mathrm{DLA}}/\phi = 1.20 . \tag{19}$$

Miyajima *et al.*[12] found the following scaling form from the computer simulation

$$t_c \approx \tau^{1.79} . \tag{20}$$

This should be compared to the result (19). The theoretical result is smaller than the computer simulation result. This may be due to the small-cell renormalization.

We shall consider the other type of the activity of the perimeter site: the activity of each aggregate particle decreasing exponentially with increasing time. The activity A_i of the perimeter site i is defined as follows:

$$A_i((t-t_0)/\tau) = \exp(-(t-t_0)/\tau) . \tag{21}$$

Similarly, we can obtain the renormalization equations for the surface conductance and the dimensionless time increment. We find the same scaling form and the same exponent. However, the scaling function $F(x)$ in (15) is different. The renormalization flows in the global flow diagram are a little different from each other, but the fixed points are the same. Qualitatively, the global flow diagram is consistent with Fig. 2. We find that the crossover phenomenon from DLA to DLSAW is universally independent upon the details of the activity.

III. PHASE TRANSITION BETWEEN DLA AND DLSAW

We consider here a model for DLA proposed by Bunde and Miyajima,[13] in which a fraction P of the particles have an infinite reaction time (as in the Witten-Sander model), with the remaining fraction $1-P$ having a finite reaction time τ_0, i.e.,

$$\tau = \begin{cases} \infty & \text{with probability } P \\ \tau_0 & \text{with probability } 1-P . \end{cases} \tag{22}$$

This model reduces to the Witten-Sander model for $P=1$ and to the model discussed by Miyajima *et al.*[12] for $P=0$. We consider the bond percolation. Each bond is randomly assigned an infinite reaction time (with probability P) or a finite reaction time (with probability $1-P$). The activity A_i on the perimeter bond i is given by

$$A_i = \begin{cases} 1 & \text{with probability } P \\ A_i(\Delta t^*) & \text{with probability } 1-P , \end{cases} \tag{23}$$

where $A_i(\Delta t^*)$ is given by Eq. (1). The growth probability p_i on the perimeter bond i is given by Eq. (3) with Eq. (23).

Similarly to Sec. II, we describe the DLA problem in terms of the dielectric breakdown model. We consider the renormalization procedure on the diamond hierarchical lattice. We make use of a three-parameter renormalization-group method. We can derive the three renormalization-group equations for the surface conductance σ_s, the dimensionless time increment Δt^*, and the probability P:

$$\sigma_s' = R_s(\sigma_s, \Delta t^*, P) , \tag{24}$$
$$\Delta t^{*\prime} = R_t(\sigma_s, \Delta t^*, P) , \tag{25}$$
$$P' = R_P(\sigma_s, \Delta t^*, P) . \tag{26}$$

We consider the renormalization of the probability P. The renormalized probability P' is given by the probability in which a cell is connected by bonds of the infinite reaction time between the bottom and the top. The probability P is consistent with the occupation probability in the bond percolation. The renormalized probability P' is given by[20]

$$P' = R_P(P) = 2P^2 - P^4 . \tag{26'}$$

As in Sec. II, we can derive the renormalization-group equations (24) and (25). The renormalization equations (24) an (25) are almost the same except for the following. The configurational probability C_α is replaced with

$$C_c = C_b[P\bar{p}_{b,2} + (1-P)p_{b,2}] , \tag{6'}$$

where $\bar{p}_{b,2}$ and $p_{b,2}$ are, respectively, the growth proba-

bilities with the infinite and the finite reaction times. The growth probabilities of Eqs. (7) are given by replacing Eq. (3) with Eq. (23). The configurational probability C_1 is replaced with

$$C_1 = C_0[P\bar{p}_{b,1} + (1-P)p_{b,1}]C_b \ . \tag{8'}$$

Thus we can obtain the three-parameter renormalization-group equations (24)–(26) explicitly. We find the six nontrivial fixed points $(0,1/\sigma_{\rm DLSAW},1)$, $(1,1/\sigma_{\rm DLA},1)$, $(P_c,1/\sigma_{\rm DLA},0)$, $(P_c,1/\sigma_c,1)$, $(0,1/\sigma_{\rm DLA},0)$, and $(1,1/\sigma_{\rm DLA},0)$ in the three-parameter space $(P,1/\sigma_s,\Delta t^*/(1+\Delta t^*))$, where $\sigma_{\rm DLSAW}$, $\sigma_{\rm DLA}$, and σ_c are, respectively, the values of the surface conductance at the fixed points. We call the six fixed points the DLSAW point, the DLA point, the percolation point, the pseudo-percolation-point, and the two pseudo-DLA-points, respectively. To find the global flow diagram in the two-parameter space $(P,\Delta t^*/(1+\Delta t^*))$, we choose a point in the parameter space, and calculate the renormalized surface conductance, the renormalized dimensionless time increment, and the renormalized fraction by using (24)–(26) to find a new point $(P',\Delta t^{*'}/(1+\Delta t^{*'}))$. We repeat this process to find the next point, and continue until we approach a stable fixed point. Figure 3 shows the renormalization flows. The crossover lines can be determined by following the renormalization flows, which start from initial points very close to the percolation point. Figure 4 shows the crossover lines and the six fixed points in the three-parameter space $(P,1/\sigma_s,\Delta t^*/(1+\Delta t^*))$. We can determine the stability of the six fixed points in the three-parameter space. The DLSAW point and the DLA point are stable in every direction. The percolation point, the pseudo-percolation-point, and the two pseudo-DLA-points are unstable fixed points. Above the percolation threshold, all the renormalization flows are merged into the DLA point. Below the threshold, all the renormalization flows are merged into the DLSAW point. We find the morphological phase transition between the DLA fractal and the DLSAW fractal at the percolation threshold. The fractal dimensions of the DLA fractal and the DLSAW fractal are given by Eq. (17). The structure of the aggregate forming at the percolation threshold consists of the mixture which is constructed by the DLA fractal on the incipient infinite cluster and the DLSAW on the remaining finite clusters. The fractal dimension of the aggregate at the percolation threshold is given by

$$d_c = P_c d_{\rm DLA} + (1-P_c)d_{\rm DLSAW} = 1.25 \ , \tag{27}$$

where $P_c = 0.618$ is the critical percolation probability on the diamond hierarchical lattice.[20] We call the aggregate at the percolation threshold the critical fractal. Above the percolation threshold there is a characteristic length

$$\xi_P \approx (P-P_c)^{-\nu} \ , \tag{28}$$

where ν is the correlation length exponent of the percolation and $\nu = 1.63$ on the diamond hierarchical lattice.[20] The structure of the aggregate becomes the critical fractal on smaller length scales $r < \xi_P$, and the DLA fractal on larger length scales $r > \xi_P$. We propose the scaling ansatz above the threshold,

$$M(r,(P-P_c)) = r^{d_c} F((P-P_c)r^{1/\nu}) \text{ if } P > P_c \ , \tag{29}$$

with

$$F(x) \approx \begin{cases} 1 & \text{if } x \ll 1 \\ x^{(d_{\rm DLA}-d_c)\nu} & \text{if } x \gg 1 \ . \end{cases} \tag{30}$$

Below the threshold, there are two characteristic lengths

$$\xi_P \approx (P_c - P)^{-\nu} \ , \qquad r_c \approx \tau^{1/\phi} \ . \tag{31}$$

If $\xi_P \gg r_c$, the crossover occurs from the critical fractal

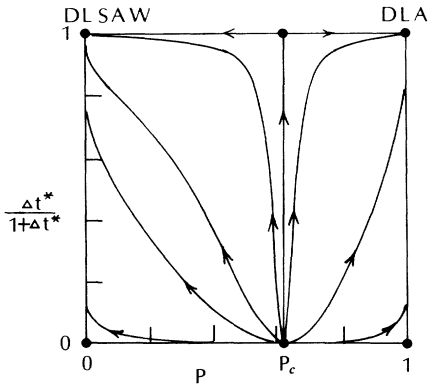

FIG. 3. Global flow diagram in the two-parameter space $(P,\Delta t^*/(1+\Delta t^*))$. Above the percolation threshold, all the renormalization flows are merged into the DLA point. Below the threshold, all the renormalization flows are merged into the DLSAW point. The geometrical phase transition between the DLA and DLSAW occurs at the percolation threshold.

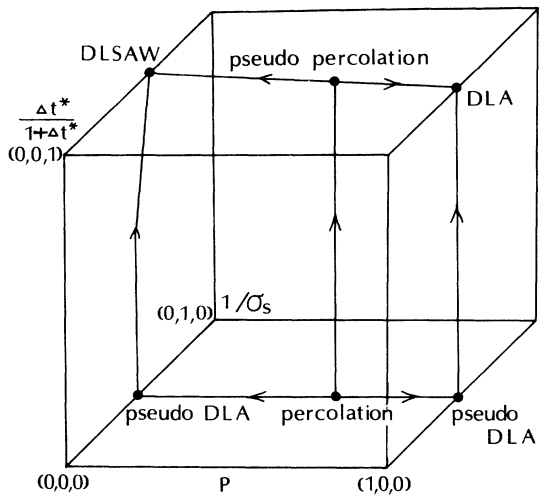

FIG. 4. Crossover lines and the six fixed points in the three-parameter space $(P,1/\sigma_s,\Delta t^*/(1+\Delta t^*))$. The DLSAW point and the DLA point are stable in every direction. The percolation point, the pseudo-percolation-point, and the two pseudo-DLA-points are unstable fixed points.

to the DLSAW fractal. However, if $\xi_P \ll r_c$, the double-crossover phenomenon occurs from the critical fractal, through the DLA fractal, to the DLSAW fractal. The double crossover is represented by the crossover line below the percolation threshold in Fig. 4. In the three-parameter space, the crossover line is shown by the curve from the percolation point, through the pseudo-DLA-point, to the DLSAW point. Physically, the double-crossover phenomenon will appear in the condition that the reaction time τ is large and the fraction P is just below the percolation threshold. We propose the scaling ansatz along the crossover line

$$M(r,(P_c-P),\tau)=r^{d_c}F_1((P_c-P)r^{1/\nu})F_2(\tau r^{\phi}) \quad \text{if } P<P_c \ , \tag{32}$$

with

$$F_1(x)\approx \begin{cases} 1 & \text{if } x \ll 1 \\ r^{(d_{\mathrm{DLA}}-d_c)\nu} & \text{if } x \gg 1 \ , \end{cases}$$

$$F_2(x)\approx \begin{cases} 1, & \text{if } x \ll 1 \\ r^{(d_{\mathrm{DLSAW}}-d_{\mathrm{DLA}})/\phi} & \text{if } x \gg 1 \ . \end{cases}$$

The geometrical phase transition between DLA and DLSAW agrees with the simulation result by Bunde and Miyajima. The double-crossover phenomenon below the percolation threshold is not found in the computer simulation by Bunde and Miyajima. We find that the morphological transition between the DLA fractal and the DLSAW fractal is induced by the percolation transition.

IV. SUMMARY

We apply the position-space renormalization-group method to the crossover and the geometrical phase transition in the extended diffusion-limited aggregation models with reaction times which were proposed by Miyajima *et al.*[12] and Bunde and Miyajima.[13] We show the crossover from the DLA fractal to the DLSAW by the global flow diagram. We calculate the crossover exponent and compare with the simulation result by Miyajima *et al.*[12] Furthermore, we analyze the geometrical phase transition between the DLA fractal and the DLSAW fractal by using the three-parameter renormalization-group method. We show that the morphological transition is induced by the percolation transition. We present the scaling forms for the geometrical phase transition near the percolation threshold.

ACKNOWLEDGMENTS

We wish to thank Jysoo Lee for especially helpful conversations.

[1]T. A. Witten and L. M. Sander, Phys. Rev. Lett. **47**, 1400 1981); Phys. Rev. B **27**, 5686 (1983).
[2]P. Meakin, Phys. Rev. A **26**, 1495 (1983); **27**, 604 (1983); **27**, 2616 (1983).
[3]*Kinetics of Aggregation and Gelation,* edited by F. Family and D. P. Landau (North-Holland, Amsterdam, 1984).
[4]*On Growth and Form,* edited by H. E. Stanley and N. Ostrowsky (Nijihoff, The Hague, 1985).
[5]*Fractals in Physics,* edited by L. Pietronero and E. Tosatti (North-Holland, Amsterdam, 1986).
[6]H. J. Herrmann, Phys. Rep. **136**, 153 (1986).
[7]P. Meakin, in *Phase Transitions and Critical Phenomena,* edited by C. Domb and J. L. Lebowitz (Academic, New York, 1988), Vol. 12, p. 336.
[8]R. Julien and R. Botet, *Aggregation and Fractal Aggregates* (World Scientific, Singapore, 1987).
[9]J. Feder, *Fractals* (Plenum, New York, 1988).
[10]*Random Fluctuations and Pattern Growth,* edited by H. E. Stanley and N. Ostrowsky (Kluwer Academic, Dordrecht, 1988).
[11]T.Vicsek, *Fractal Growth Phenomena* (World Scientific, Singapore, 1989).
[12]S. Miyajima, Y. Hasegawa, A. Bunde, and H. E. Stanley, J. Phys. Soc. Jpn. **57**, 3376 (1988).
[13]A. Bunde and S. Miyajima, Phys. Rev. A **38**, 2099 (1988).
[14]R. M. Bradley and D. Kung, Phys. Rev. A **34**, 723 (1986).
[15]J. Lee, A. Coniglio, and H. E. Stanley, Phys. Rev. A **41**, 4589 (1990).
[16]T. Nagatani, Phys. Rev. A **40**, 7286 (1989).
[17]T. Nagatani and H. E. Stanley, Phys. Rev. A **41**, 3263 (1990).
[18]T. Nagatani, Phys. Rev. A **36**, 5812 (1987); **38**, 2632 (1988).
[19]L. A. Turkevich and H. Scher, Phys. Rev. Lett. **55**, 1026 (1985).
[20]D. C. Hong, J. Phys. A **17**, L929 (1984).